HYDJET++ simulations and reconstruction of the anisotropic flow in Pb+Pb collisions at the LHC

L.V. Bravina, G.Kh. Eyyubova^{*ab}**, E.E. Zabrodin**^{ab}
[a] *Universitetet i Oslo, Norway*
E-mail: `gyulnare@student.matnat.uio.no`

V.L. Korotkikh, I.P. Lokhtin, L.V. Malinina, S.V. Petrushanko, A.M. Snigirev
[b] *M.V. Lomonosov Moscow State University, D.V. Skobeltsyn Institute of Nuclear Physics, 119991, Moscow, Russia*
E-mail: `vlk@lav01.sinp.msu.ru`

The azimuthal anisotropy of charged particles in heavy ion collisions is an important probe of quark-gluon plasma evolution at early stages. In the present paper the elliptic flow pattern in Pb+Pb collisions at $\sqrt{s_{NN}} = 5.5$ TeV is analyzed for different hadron species in the frameworks of HYDJET++ Monte-Carlo model. The influence of resonance decays on particle flow is investigated. The different methods of elliptic flow reconstruction are compared under LHC conditions.

High-pT Physics at LHC -09
February 4- 7 2009
Prague, Czech Republic

---

[*] Speaker.

PoS(High-pT physics09)047

1. Introduction

In non-central collisions between two nuclei the beam direction and the impact parameter vector define a reaction plane for each event. The observed particle yield versus azimuthal angle with respect to the event-by-event reaction plane gives information on the early collision dynamics [1, 2]. An initial nuclear overlap region has an “almond” form at non-zero impact parameter. If the produced matter interacts and thermalizes, pressure is built up within the almond shaped region leading to anisotropic pressure gradients. This pressure pushes against the outside vacuum and the matter expands collectively. The result is an anisotropic azimuthal angle distribution of the detected particles. One can expand this azimuthal angle distribution in a Fourier series. The second coefficient of the expansion v_2 is called the elliptic flow.

It was found [2, 3] that anisotropic flow is self-quenching phenomenon since it reduces spatial anisotropy as it evolves. Therefore, observed elliptic flow must originate at early stages of the collision when the anisotropy is still present in the system. There is no elliptic flow generated when the spherical symmetry is restored in the system. Thus the elliptic flow keeps information about hot and dense matter created in relativistic heavy ion collisions.

As the fireball expands, its temperature and energy density drop. Finally, at the freeze-out stage, the system breaks up into hadrons and their resonances. The effect of resonance decays, i.e. final state interaction, on the resulting elliptic flow of particles is quite important. For instance, it can explain partly the observed deviation of pion elliptic flow from the so-called constituent quark scaling [4]. The exact resonance decay kinematics at very low momenta can probably be accounted for the reduction of v_2 coefficient for pions at midrapidity in the hydrodynamical calculation [5].

In this work we employ the HYDJET++ model [6, 7] to estimate the azimuthal anisotropy of particles in Pb+Pb collisions at LHC energy and to study the influence of resonance decays, jet production and jet quenching on elliptic flow, and also to test the different methods of v_2 restoration for different particles.

2. Simulation of elliptic flow with HYDJET++ model

The HYDJET++ model [6, 7] represents a superposition of soft and hard parts. These parts are independent and their contribution to the total multiplicity production depends on collision energy, centrality and is tuned by model parameters. The hard part of the model is identical to the hard part of the HYDJET model [8] and has the possibility to account for jet quenching effect. The soft part of HYDJET++ event represents the "thermal" hadronic state where multiplicities are determined under assumption of thermal equilibrium [9]. Hadrons are produced on the hypersurface represented by a parametrization of relativistic hydrodynamics with given freeze-out conditions. Feed down of hadronic resonances is taken into account. HYDJET++ is capable of reproducing the bulk properties of heavy ion collisions at RHIC, i.e. hadron spectra and ratios, radial and elliptic flow, femtoscopic momentum correlations, as well as high-p_T hadron spectra [6, 7].

Fig. 1 presents the impact parameter b dependence of the elliptic flow coefficient v_2 of charged particles. The coefficient v_2 is defined here as the cosine of twice the azimuthal angle of a particle relative to the reaction plane angle Ψ_R (which is known in each simulated event), and averaged over all charged hadrons in each event, $v_2 = \langle \cos(2\varphi - \Psi_R) \rangle$. As expected, the elliptic flow coefficient

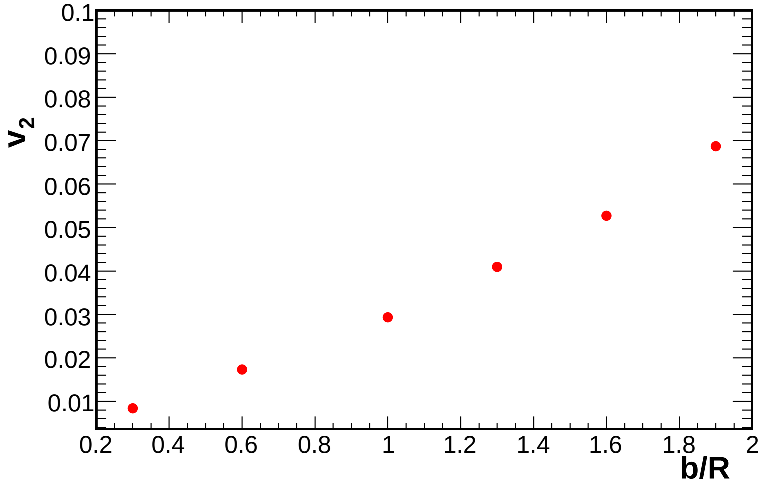

Figure 1: The impact parameter dependence of elliptic flow in HYDJET++ model for Pb+Pb collisions at LHC energy.

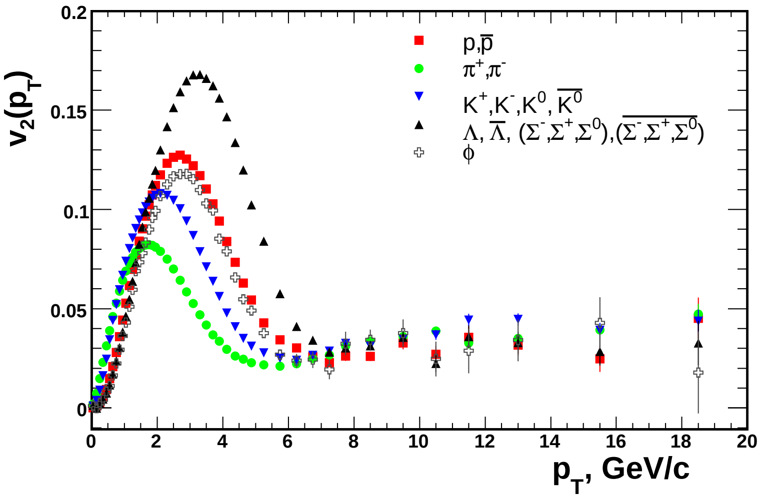

Figure 2: The p_T-dependence of elliptic flow in HYDJET++ model for different hadron species produced in Pb+Pb collisions at $\sqrt{s_{NN}} = 5.5$ TeV with centrality 42%.

grows with increasing impact parameter (i.e. with increasing of azimuthal anisotropy of initial nuclear overlap region). Further we consider elliptic flow at fixed centrality, $\sigma/\sigma_{geo} = 42\%$ ($b \approx 1.3R$). Fig. 2 shows the p_T dependence of elliptic flow coefficient for most abundant hadrons, i.e. pions, kaons, protons, lambdas and sigmas. This behavior of elliptic flow can be explained in following way. The flow of hydro part rises monotonically up to $v_2 \simeq 0.5$ at $p_T \simeq 6$ GeV/c while the relative contribution of hydro part to particle multiplicity decreases with p_T, so the particles with $p_T \gtrsim 6$ GeV/c are produced only through jets (hard part). The flow of the jet part is close to zero in this p_T range. It results in initial rise of $v_2(p_T)$ followed by the fall off at $p_T \gtrsim 3$ GeV/c. The jet part at $p_T \gtrsim 7$ GeV/c also presents some amount of flow ($\approx 4\%$) at the LHC energies due to jet quenching effect. The energy loss of the high p_T partons depends on the passing length of

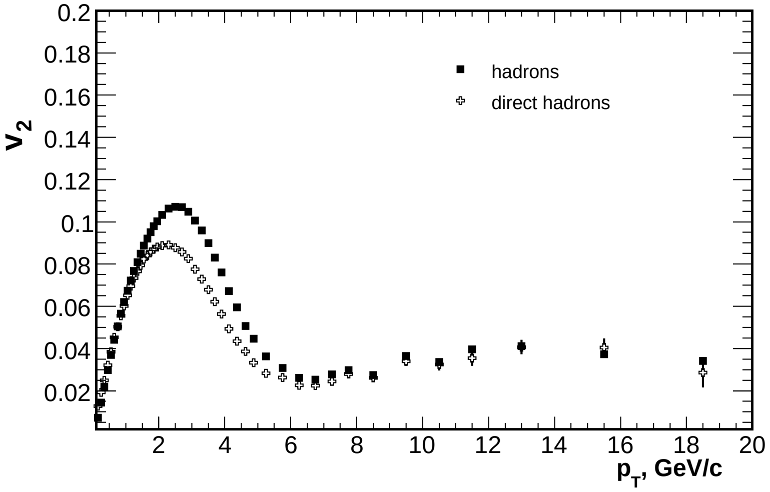

Figure 3: The p_T-dependence of elliptic flow in HYDJET++ model produced in Pb+Pb collisions for all hadrons and for direct hadrons at $\sqrt{s_{NN}} = 5.5$ TeV with centrality 42%.

the anisotropic matter thus giving the different yield of the high-p_T partons in the in-plane (x,z) and out-of plane (y,z) directions.

The pronounced feature of the RHIC experimental data [10] reproduced by HYDJET++ in Fig. 2 is the crossing of baryon and meson branches. In HYDJET++ at low p_T the hydro part dominates and the flow is strictly ordered by particle masses. The lighter particles (pions, kaons) have the larger flow than heavier (protons, lambdas).

The slope of the heavy particles p_T-spectra is steeper then one of the light particles, as a result the hydro part dominates till larger p_T values for heavier particles: i.e. for pions hydro dominates till ~ 4 GeV/c, for protons it dominates till ~ 5 GeV/c. As a result at $p_T > 4$ GeV/c the mass ordering changes on the opposite: the heaviest particles have the largest flow.

The influence of resonance decays. At RHIC energies the transition from baryon rich matter to meson reach matter was found. As was predicted by Hagedorn, at high energies most of the particles will be produced through resonance decays with shifting of the average mass to heavier sector. The effect of resonance decays should be accounted for when one considers the v_2/n_q scaling. Table 1 shows the contributions of direct and resonant production for various hadron species including feed down from weak decays for our Pb+Pb event sample generated with HYDJET++ at LHC energies. One can see that 80% of pions, 70% of protons, 61% of Σ and Λ-hyperons and 56% of kaons are produced from resonance decays. Figures 3 and 4 display difference between v_2 of all these hadrons and v_2 of only direct hadrons. A degree of the influence of resonance decays on elliptic flow coefficient is quite different for various hadrons. The effect is strongest for protons; rather moderate for Σ and Λ-hyperons and pions; and negligible for kaons.

Let us consider the case of pion and proton flow. The relative contribution from resonance decays for them is presented in Table 2. Fig. 5 shows differences in secondary pions and protons from (anti)deltas ($\Delta^{++}, \Delta^{+}, \Delta^{0}, \Delta^{-}$) decays. Because of the kinematics of decay, when heavy baryon resonance decays into secondary baryon plus pion, the most part of its momentum is carried by the baryon while the pion is produced with low p_T. Thus, the pion elliptic flow gets an extra boost

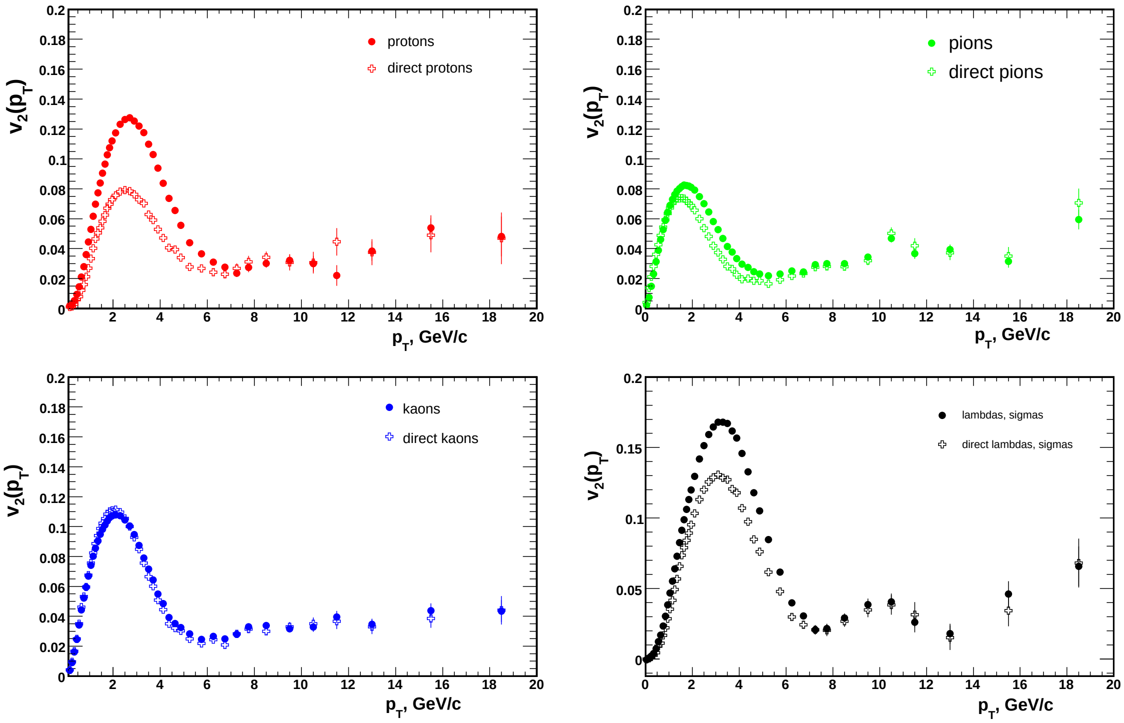

Figure 4: The same as Fig. 2, but for protons (upper left), pions (upper right), kaons (bottom left), lambdas plus sigmas (bottom right).

Table 1: Yields of the particles produced directly and with resonance decays at midrapidity region, c=42%. Weak decays of the strange particles are included.

	$\pi^{\pm}$	$K+\bar{K}$	$p+\bar{p}$	$\Lambda+\bar{\Lambda}+\Sigma+\Sigma$	ϕ
all	860	185	63.8	42.3	6.55
direct	169	81.4	18.6	14.2	6.5
direct %	20 %	44 %	30 %	39 %	99 %

Table 2: Yields of the pions and protons produced directly and from resonance decays in HYDJET++, c=42%.

	direct	ρ-decay	K^0-decay	ω-decay	Λ-decay	Δ-decay
$\pi^{\pm}$	22%	26%	16%	11%	2.3%	1.8%
$p,\bar{p}$	30%	-	-	-	27%	15%

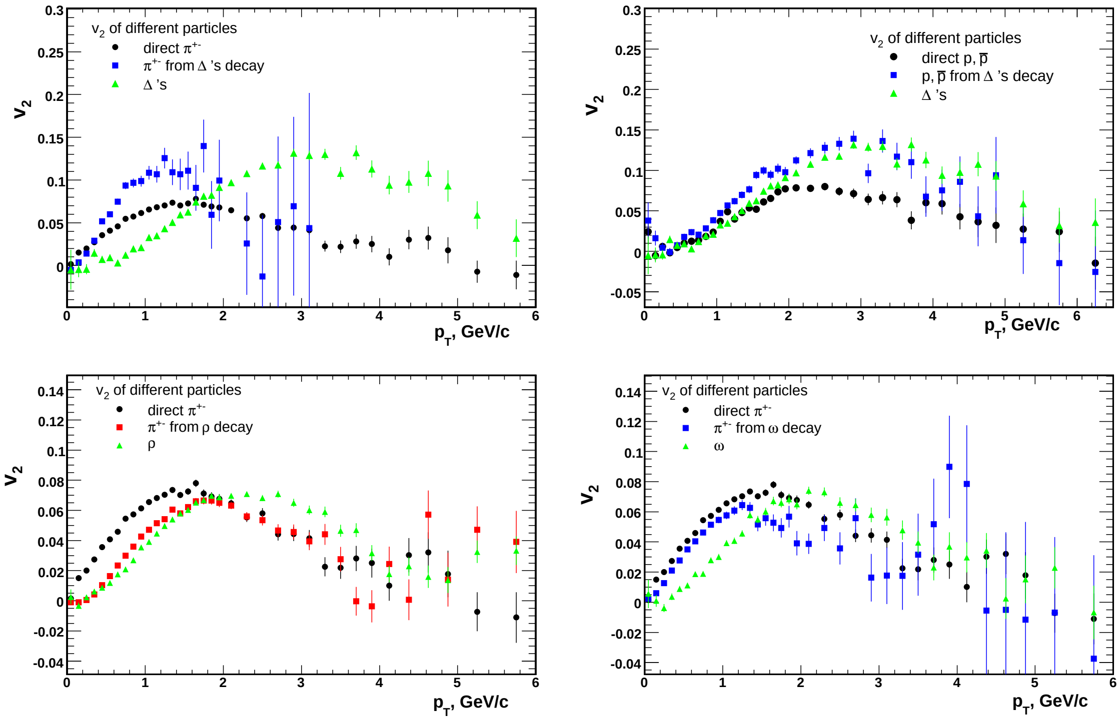

Figure 5: Top: The p_T-dependence of elliptic flow for pions (left) and (anti)protons (right) coming from Δ decays. Bottom: The elliptic flow p_T-dependence of pions coming from ρ decays (left) and ω decays (right).

at low p_T from the flow of heavy resonances (Fig. 5, top left). On the other hand, the secondary baryon carries practically the same $v_2(p_T)$ as mother particle (Fig. 5, top right). Note, that most of secondary pions are produced from ρ- and ω-mesons. But momentum distribution for ρ-meson and for secondary pions are quite close, thus the $v_2(p_T)$ almost coincides for them (Fig 5, bottom left). The influence of heavy resonance decays on pions flow at $p_T \lesssim 2$ GeV/c is effectively compensated by influence of ρ-decays. For higher p_T the contribution from K-decay determines the observed excess of the pion flow over direct pion flow.

The secondary protons come from Λ and Δ decays in approximately equal proportions. They predominantly possess the flow of these resonances, as can be seen from top left Fig. 4.

One can see from Fig. 5 that hadrons produced from resonance decays carry the same amplitude of v_2 as that of the mother particle but the maximum may be shifted to the soft p_T region. Elliptic flow of pions from the $\rho \to \pi\pi$ decay almost coincides with v_2^{ρ} (Fig. 5, bottom left) while in 3-particle decay $\omega \to \pi\pi\pi$ pions are getting obviously softer p_T distribution, thus their elliptic flow is transferred to the softer p_T region compared with $v_2^{\omega}(p_T)$ (Fig. 5, bottom right).

Therefore, contributions from resonances sometimes increase and sometimes decrease initial elliptic flow of directly produced pions. This effect, especially pronounced at LHC energy, can lead to violation of the mass-hierarchy in the $v_2(p_T)$ sector.

3. Reconstruction of elliptic flow at the LHC

There exists a wealth of anisotropic flow measurement methods, each having its own advantages and limitations. Here we apply three wide-spread methods to calculate the v_2 coefficient. One of them uses the event plane angle determination, and others are cumulant and Lee-Yang zero methods.

The event plane angle, Ψ_n, can be determined from the measured n-th harmonics via the standard method [11, 12]:

$$\tan n\Psi_n = \frac{\sum\limits_i w_i \sin(n\varphi_i)}{\sum\limits_i w_i \cos(n\varphi_i)}, \qquad n \geq 1, \quad 0 \leq \Psi_n < 2\pi/n, \tag{3.1}$$

where φ_i is the azimuthal angle of the i-th particle and w_i is the weight. The sum runs over all particles in given event. The observed value of $v_2^{\rm obs}$ is calculated using the event plane (EP) method by the formula:

$$v_2^{\rm obs}\{EP\} = \langle \cos 2(\varphi - \Psi_2) \rangle, \tag{3.2}$$

where event plane angle Ψ_2 is the estimate of the true reaction plane angle Ψ_R, the mean was taken over all charged particles in a given event and then over all events. Usually the true elliptic flow coefficient is evaluated by dividing $v_2^{\rm obs}$ by the factor R [12], which accounts for the event plane resolution:

$$v_2\{EP\} = \frac{v_2^{\rm obs}\{EP\}}{R} = \frac{v_2^{\rm obs}\{EP\}}{\langle \cos 2(\Psi_2 - \Psi_R) \rangle}. \tag{3.3}$$

This procedure relies on the assumption that there are no non-flow correlations (e.g., correlations due to momentum conservation, quantum statistics, resonance decays, jet production) or that they are negligible, and also that the full event multiplicity is large enough. Generally such assumptions are not true. Studying these effects in real data is a separate and non-trivial task.

In order to avoid the trivial autocorrelation of particles the event plane angle Ψ_2 and hence R are calculated in one angular distribution sample of event, and v_2 in another sample with the same multiplicity. The samples may be selected in two regions of pseudorapidity $\eta < 0$ and $\eta > 0$.

The basic idea of the cumulant method is that the v_2 coefficient can be expressed in terms of particle azimuthal correlations [13, 14]. The procedure is to construct two-particle correlator or cumulant

$$\begin{aligned} v_2\{2\}^2 = \langle \cos 2(\varphi_i - \varphi_j) \rangle &= \langle \cos 2((\varphi_i - \Psi_R) - (\varphi_j - \Psi_R)) \rangle \\ &\simeq \langle \cos 2((\varphi_i - \Psi_R) \rangle \langle (\varphi_j - \Psi_R)) \rangle. \end{aligned} \tag{3.4}$$

As in the first method it is necessary to exclude the autocorrelations. The approximative equation in the last string of Eq. (3.4) means that the non-flow correlations are small.

The two-cumulant method can be extended to the case of many-particle correlations [14]. It is known as the higher order cumulant method or the method with Lee-Yang zeroes. The higher order cumulant methods are less sensitive to non-flow effects. The Lee-Yang zeroes method [15] refers to the Generation function as a complex function of variable r:

$$G^\theta(ir) = \langle e^{irQ^\theta} \rangle, \tag{3.5}$$

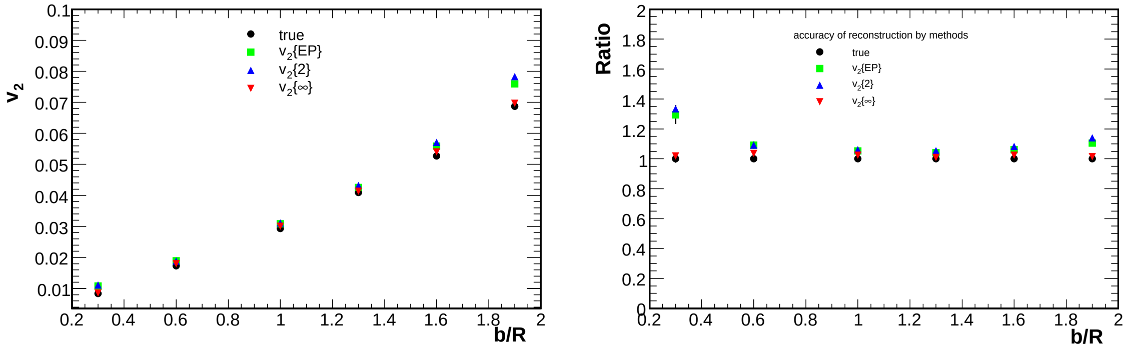

Figure 6: (a) The *b*-dependence of elliptic flow in HYDJET++ model for Pb+Pb at LHC energies reconstructed by different methods.(b) The ratio of the methods to the true value.

where Q^{θ} is the flow vector and θ is arbitrary angle.

$$Q^{\theta} = \sum_{j}^{M} \cos 2(\varphi_j - \theta). \tag{3.6}$$

The integral v_2 value is connected with the first minimum of module of the Generation function $|G^{\theta}(ir)|$,

$$v_2^{\theta}\{\infty\} \equiv \frac{j_{01}}{M r_0^{\theta}}, \tag{3.7}$$

where $j_{01} = 2.405$ is the first root of the Bessel function $J_0(x)$. The differential value is given by more complex expression:

$$\frac{v_2^{\theta}(p_T)\{\infty\}}{M v_2\{\infty\}} \equiv Re\left(\frac{\langle \cos 2(\varphi - \theta) e^{i r_0^{\theta} Q^{\theta}} \rangle}{\langle Q^{\theta} e^{i r_0^{\theta} Q^{\theta}} \rangle}\right). \tag{3.8}$$

The natural resolution parameter that appears in these methods is $\chi \sim v_2\sqrt{M}$, i.e. methods depend both on strength of the flow v_2 and on multiplicity M. The flow increases with rise of the impact parameter while the multiplicity decreases. The best reliability of the methods is achieved at midcentral collision (Fig. 6). The overestimation of the true elliptic flow by $v_2\{EP\}$ and $v_2\{2\}$ methods in most central and peripheral collision is up to 30%. This is due to nonflow correlations. We see that the Lee-Yang zeroes method is good enough to reconstruct v_2 in large centrality range except very peripheral collisions where the multiplicity is too small.

The origin of nonflow correlation is mostly due to jets. It can be revealed from Fig. 7 where the event plane method severely overestimates the original elliptic flow at high p_T. The possibility of v_2 reconstruction for different hadron species based on the generalization of Lee-Yang zeroes method [16, 17] at the LHC is under investigation.

4. Conclusion

The elliptic flow pattern in Pb+Pb collisions at $\sqrt{s_{NN}} = 5.5$ TeV is analyzed for different hadron species in the frameworks of HYDJET++ Monte-Carlo model. Resonance decays and in-medium jet fragmentation result in the smearing of hydro-induced mass-ordering of elliptic flow

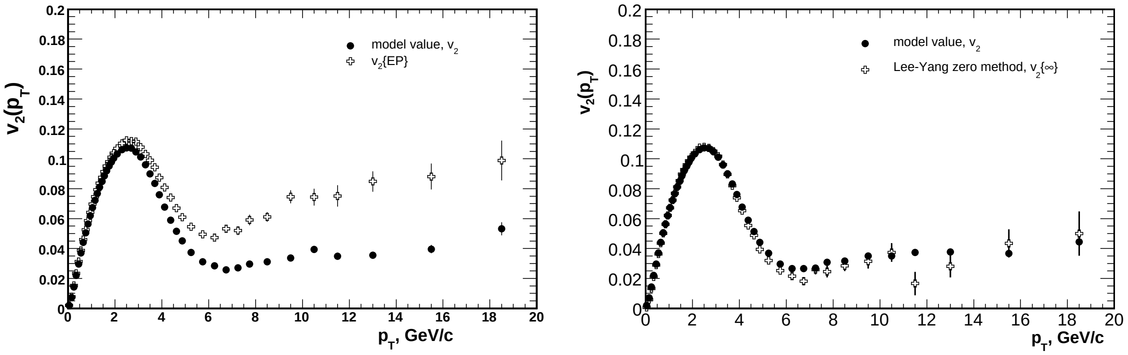

Figure 7: The p_T-dependence of elliptic flow in HYDJET++ model for Pb+Pb at LHC energies reconstructed by Event plane method (left) and Lee-Yang zeroes method (right). Centrality is 42%, charged hadrons.

coefficients v_2 for different hadron species in low- and high-p_T domains, respectively. Increase of v_2 due to resonant production is strongest for protons, moderate for Σ and Λ-hyperons and pions, and negligible for kaons. The total effect on a given particle specie may contain two different contributions, either increasing or decreasing the direct flow $v_2(p_T)$, as we saw on pion example.

The comparison between three different methods of elliptic flow reconstruction under LHC conditions has been performed. The event plane, the two-particle correlation and Lee-Yang zeroes methods show the different restoration power. The event plane and two-particle correlation methods work well for low-p_T region where jet influence is negligible, while Lee-Yang zeroes method is able to remove non-flow (jet) correlations at high p_T.

This work was supported, in part, by the QUOTA Program, Norwegian Research Council (NFR) under contract No 185664/V30, Russian Foundation for Basic Research (grants No 08-02-91001 and No 08-02-92496), Grants of President of Russian Federation (No 107.2008.2 and No 1456.2008.2) and Dynasty Foundation.

References

[1] J.-Y. Ollitrault, *Phys. Rev.* **D 46**, (1992) 229.

[2] H. Sorge, *Phys. Rev. Lett.* **82**, (1999) 2048.

[3] P. F. Kolb, U. W. Heinz, *Quark qluon Plasma 3*, World Scintific, Singapore 2003 [arXiv:nucl-th/0305084].

[4] V. Greco and C. M. Ko, *Phys. Rev.* **C 70** (2004) 024901.

[5] T. Hirano, *Phys. Rev. Lett.* **86** (2001) 2754.

[6] I.P. Lokhtin, L.V. Malinina, S.V. Petrushanko, A.M. Snigirev, I. Arsene and K. Tywoniuk, *Comput. Phys. Commun.* **180** (2009) 779.

[7] I.P. Lokhtin et al., in this Proceedings, `arXiv:0903.0525`.

[8] I.P.Lokhtin and A.M.Snigirev, *Eur. Phys. J.* **C 46**,(2006) 211.

[9] N.S. Amelin et.al, *Phys. Rev.* **C 74**, (2006) 064901; *Phys. Rev.* **C 77**, (2008) 014903.

[10] A. Adare et al. [PHENIX Collaboration], *Phys. Rev. Lett.* **98**, (2007) 162301.

[11] S. A. Voloshin and Y. Zhang, *Z. Phys.* **C 70**,(1996) 665.

[12] A. M. Poskanzer and S. A. Voloshin, *Phys. Rev.* **C 58**,(1998) 1671.

[13] S. Wang et al., *Phys. Rev.* **C 44** (1991) 1091 .

[14] N. Borghini, P.M. Dinh and J.-Y. Ollitrault, *Phys. Rev.* **C 64**, (2001) 054901.

[15] R. S. Bhalerao, N. Borghini, J.-Y. Ollitrault, *Nucl. Phys.* **A 727**, (2003) 373.

[16] N. Borghini, R.S. Bhalerao, J.-Y. Ollitrault, *J*.Phys. G **30** (2004) S1213.

[17] B.I. Abelev et al. [STAR Collaboration], *Phys. Rev.* **C 77** (2008) 054901.